

Characterisation of the Chemical Reactivity of a CaCO_3 Powder for Its Decomposition

Vincent Bouineau, Michèle Pijolat* and Michel Soustelle

Centre SPIN-CRESA, Ecole des Mines de Saint-Etienne, 158 Cours Fauriel, 42023 Saint-Etienne Cedex, France

Abstract

The decomposition of calcium carbonate has been studied by isothermal and isobaric thermogravimetry at 700°C, under various pressures of carbon dioxide. The kinetic curves, which have a sigmoidal shape, have been interpreted with a model involving nucleation and growth processes based on the Mampel's model. It was supposed that nucleation occurs at the surface of all the particles and that growth proceeds isotropically inward in each of them. This model allowed to characterise the chemical reactivity of several CaCO_3 powders by means of the determination of both their specific nucleation frequency and their specific growth rate. © 1998 Elsevier Science Limited. All rights reserved

1 Introduction

The formation of CaO from the thermal decomposition of a CaCO_3 powder depends both on its textural characteristics (which are related to the distribution in shape and size of the particles) and the intrinsic chemical reactivity (which depends chiefly on the amount and nature of impurities). Previous studies of the decomposition of calcium carbonate have shown that the reaction involves the competition of nucleation and growth processes in agreement with a sigmoidal shape of the isothermal curves.^{1,2} The kinetic analysis was done considering the decreasing part of the corresponding rate curve on the basis of the sphere contracting model, and thus did not take into account the nucleation step which is responsible for the initial accelerating part of the curves. In the present work, we propose to characterise the intrinsic chemical reactivity of the powder by means of the determination of the specific nucleation frequency and the specific growth rate for a series of CaCO_3 powders

versus CO_2 pressure at 700°C. We present a kinetic model that differs from the Mampel's model^{3,4} by the fact that all the particles of the powder contribute to the surface at which the nuclei may statistically appear.

2 Experimental

2.1 Samples

Samples of calcium carbonate were supplied by Lhoist: one (S) was synthesised by precipitation of calcium oxide and carbon dioxide, while four others (G, R, B, D) were natural limestones with various amounts and types of impurities as reported in Table 1. All the samples present the calcite structure.

The powders were sieved in order to obtain a monomodal distribution in size of the selected particles. The scanning electron microscopy (JEOL JSM-840) indicated that in all the initial powders the particles are single crystalline⁵ and their shape could rather well be considered as spherical. Thus we calculated for each powder a statistical mean radius from the specific surface area, as determined from the BET method using a Micromeritics ASAP2000. The values of the surface area and the corresponding mean size of the samples are reported in the third and fourth columns of Table 1, respectively.

2.2 Thermogravimetry analysis

The extent of conversion, ξ , versus time was obtained by means of isothermal and isobaric thermogravimetry (TG), under static CO_2 atmosphere. Samples (ca 5 mg) were placed in a thermobalance Setaram MTB 10-8. Then the thermobalance was rapidly evacuated to a pressure near 1 Pa and filled at room temperature with carbon dioxide to around 5333 Pa, which is higher than the equilibrium pressure of the transformation. Then the furnace, which was preheated at 700°C in a low position, could be manually raised at the level of the sample. While the temperature of

*To whom correspondence should be addressed.
E-mail: mpijolat@emse.fr

Table 1. Impurities, specific surface area and mean statistical radius of the samples of calcium carbonate

Sample	Impurities	Area ($m^2 g^{-1}$)	r_0 (μm)
S	Fe ₂ O ₃ and MgCO ₃ (~150 ppm)	7.6	0.6
G	Fe ₂ O ₃ (~30 ppm) and MnO (< 5 ppm)	1.0	4.6
R	Fe ₂ O ₃ and MgCO ₃ (~150 ppm)	2.4	1.8
B	SiO ₂ (< 2%) and Al ₂ O ₃ (< 2%)	1.9	2.4
D	SiO ₂ (~2 to 3%) Al ₂ O ₃ (~2 to 3%)	2.7	1.6

the sample was increasing, there was a slight mass loss due to the desorption of water. Once the temperature of the sample was stabilised at 700°C, the carbon dioxide pressure in the thermobalance was decreased to that of the experiment in order to begin the decomposition. The time 'zero' of the TG curves is taken just at this moment. The TG curves were converted into the kinetic curves $\xi(t)$ and $\alpha(t)$ using eqns (1) and (2):

$$\xi(t) = n_0 \alpha(t) \quad (1)$$

$$\alpha(t) = \Delta m(t) / \Delta m_f \quad (2)$$

in which n_0 is the initial number of mole of calcium carbonate, $\Delta m(t)$ is the mass loss at time t , Δm_f is the final total mass loss. The total mass loss for each sample was found to be in agreement with the theoretical one. For example in the case of the D sample, the mass loss was 41.2% of the initial one, that was attributed to the presence of 6.4% of impurities in, which is in agreement with the theoretical content in Table 1.

3 Kinetic Model of Nucleation and Isotropic Growth

3.1 Nucleation and growth processes

The modelling of the decomposition of calcium carbonate is based on the competition between the processes of nucleation and growth of the new phase, the calcium oxide, which nucleates at the surface of the initial particles. If we suppose that the rate limiting step of the growth process is located at the interface between the two phases, whose extent of area for the whole powder is noted S_I , and if S_L represents the extent of the surfaces of the particles not yet covered with calcium oxide, then the absolute rate of conversion, $d\xi/dt$ is given by the following expression:

$$\frac{d\xi}{dt} = \nu S_I + g S_L \quad (3)$$

in which ν and g are, respectively, the specific rates of growth and of nucleation, whose unit is mole

$m^2 s^{-1}$. In practice it is more convenient to use the specific frequency of nucleation, γ , which is the number of nuclei that appear by meter square and by second, related to the specific nucleation growth according to eqn (4):

$$g = \gamma N_c \quad (4)$$

in which N_c is the number of mole of calcium oxide per nucleus, which is obviously unknown.

According to the assumption about the location of the rate-limiting step of the growth process, and due to their definition, the specific rate of growth, as well as the specific frequency of nucleation are not dependant on time nor on the geometrical aspect of the particles in the powder. However, they do vary with the intensive variables of the system like temperature, partial pressure in CO₂, impurity content, etc. For these reasons, their knowledge will provide us with the intrinsic chemical reactivity of a sample, whatever the textural characteristics of the powder would be.

In practice, the amount of solid transformed in the nucleation process is small compared to that transformed by the growth of the nuclei, so the problem of the kinetic modelling of the reaction reduces to the determination of the term νS_I in eqn (3). However, the nucleation process is not neglected because the amount of interfaces created from the growth of the nuclei depends on the number of these nuclei. This can be seen on the scheme presented in Fig. 1 in the case of a single particle.

The general case of nucleation and growth has been previously described by a model first proposed by Mampel.^{3,4} This model was based on the following assumptions: (i) the initial powder is composed of spherical homodispersed particles; (ii) the nuclei which are formed on the surface are supposed to grow isotropically into the particle, what we call internal development; (iii) the rate-limiting step of growth occurs at the internal interface, (iv) the extent of conversion of the powder is identical to that of a single particle.

However, this last assumption is not necessarily verified, which has led us to propose a more general model by considering that the nuclei may appear according to the frequency γ at the surface of all the particles of the powder. If N_τ represents the number of particles without nuclei at time τ , the number of particles on which nuclei will appear during the period $d\tau$ will be:

$$-dN_\tau = 4\pi r_0^2 \gamma N_\tau d\tau \quad (5)$$

where r_0 is the initial radius of the particles.

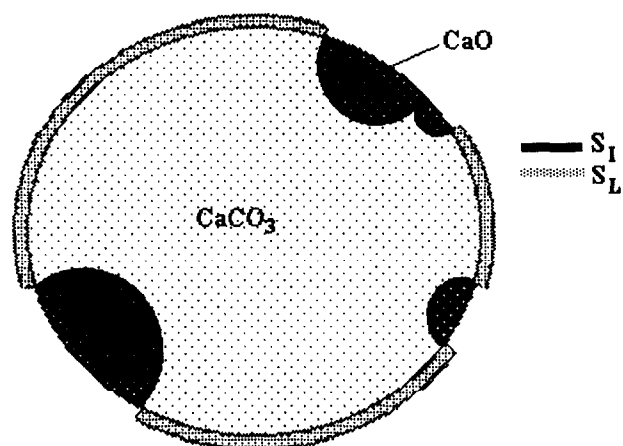


Fig. 1. Scheme of the reactional areas of nucleation (S_L) and growth (S_I) for a single particle of calcium carbonate.

Thus the number of particles that have their first nucleus at the same time τ can be obtained by integration of eqn (5) which gives:

$$-dN_\tau = 4\pi r_0^2 \gamma N_0 \exp(-4\pi r_0^2 \gamma \tau) d\tau \quad (6)$$

in which N_0 is the total number of particles in the sample. The extent of conversion of the powder can thus be obtained using, for each particle, the extent of conversion given by the Mampel's model, noted α_τ , according to the following expression:

$$\alpha(t) = 4\pi r_0^2 \gamma \int_0^t \alpha_\tau \exp(-4\pi r_0^2 \gamma \tau) d\tau \quad (7)$$

By this way the description of the transformation of the particles becomes more realistic since each of them has its own behaviour, while only two quantities characterise the chemical reactivity: γ and v .

3.2 Application of the modelling

From this model, that we will call 'generalised Mampel', it is possible to calculate the theoretical fractional conversion (α) and the theoretical rate ($d\alpha/d\theta$) as a function of a dimensionless time θ , using the same parameter A than in the Mampel's model. θ and α are defined by eqns (8) and (9):

$$\theta = \frac{V_m v}{r_0} t \quad (8)$$

$$A = \frac{4\pi r_0^3 \gamma}{V_m v} \quad (9)$$

in which V_m is the molar volume of calcium carbonate.

We define the experimental and theoretical reduced rates, $\omega_{\text{exp}}(\alpha)$ and $\omega_{\text{mod}}(\alpha)$ respectively, according to eqns (10) and (11)

$$\omega_{\text{exp}}(\alpha) = \frac{\frac{d\alpha}{dt} \exp(\alpha)}{\frac{d\alpha}{dt} \exp(\alpha = 0.5)} \quad (10)$$

$$\omega_{\text{mod}}(\alpha) = \frac{\frac{d\alpha}{dt} \text{mod}(\alpha)}{\frac{d\alpha}{dt} \text{mod}(\alpha = 0.5)} \quad (11)$$

If the model correctly describes the transformation, there must exist a value of the parameter A such that the experimental and theoretical reduced rates are identical. The curve of the experimental reduced rate is thus 'fitted' by searching the best value of A : in practice a direct numerical fitting procedure was not possible, so the best agreement was considered to be obtained when both the values of α at the inflexion point, α_i , were as near as possible, and the coincidence between the two curves were acceptable. The quality of the agreement was appreciated by means of the calculation of the minimum of the sum of squared difference between the experimental and theoretical reduced rate curves.

The values of the fractional conversion at the inflexion point have been calculated and drawn versus the parameter A in Fig. 4. It is shown that, for an experimental value of α_i , higher than 0.27 two distinct values of A can be found. As the corresponding theoretical rate curves are practically the same, it is in general not possible to choose between the two values of A from the simple comparison to the experimental curve. So microscopic observations of samples at a low extent of transformation are required since a high value of A implies necessarily a high ratio γ/v and thus a large number of growing nuclei by particle, contrarily to a low value of A . The problem was already encountered with the Mampel's model in the case of the transformation of cerium hydroxycarbonate into cerium dioxide,⁴ and solved by the aid of microscopic observations. Then the linear relationship existing between θ and t according to the eqn (8) is checked by means of the corresponding $\alpha(t)$ and $\alpha(\theta)$ curves. The slope of the straight line, determined by a numerical mean square roots fit, gives the value of $V_m v/r_0$, which in turns provides us with the value of v , the specific rate of growth. It is thus possible to determine the value of the nucleation frequency, γ , using eqn (9). By this way we characterise the intrinsic chemical reactivity of the samples of calcium carbonate; moreover we may obtain for each sample the variations of v and

γ against the carbon dioxide partial pressure by modifying the experimental conditions.

4 Results

The experimental kinetic curves $\alpha(t)$ obtained at 700°C for carbon dioxide pressures from 533 to 1333 Pa, are shown in Fig. 2 in the case of the synthetic calcium carbonate (S). It can be seen that as expected the increase in the carbon dioxide pressure has an inhibiting effect on the reaction. Figure 3 displays the kinetic curves obtained at the same temperature and at 800 Pa of carbon dioxide for the samples S, G, R, B, D. It can be observed that the curves of B and R samples are identical, while G is transformed very slowly compared to the four other samples.

These kinetic curves $\alpha(t)$ were transformed into the experimental reduced rate curves $\omega_{\text{exp}}(\alpha)$ according to eqn (10). These curves exhibit a maximum for the value α_i of the inflexion point in the curve $\alpha(t)$. It has been observed from transmission electron microscopy [as shown in Fig. 5(a) and (b)] that some of the particles appear to be partially decomposed with only a few nuclei. Such a behaviour is typically that of a very low nucleation frequency, which is in favour of a low value of A . Consequently, it was decided to choose for each experiment the lowest value of A .

Figure 6 shows an example of the comparison between the experimental and theoretical reduced rates versus α , when the best value of A was found to be equal to 1.2. On the figure, the theoretical curve corresponding to the best agreement with the Mampel's model ($A = 0.8$) has also been shown in

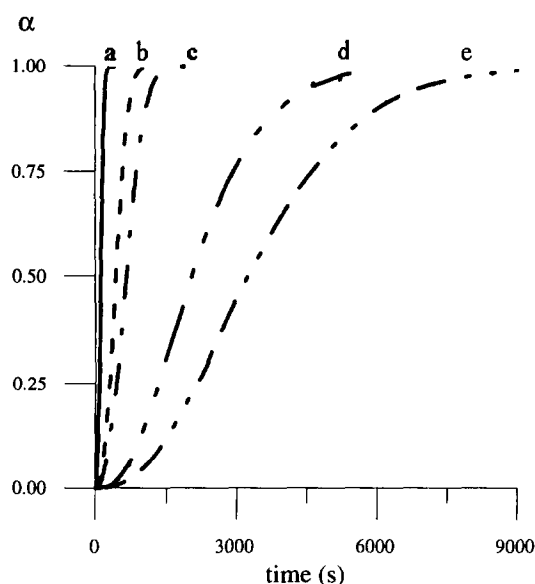


Fig. 2. Influence of the carbon dioxide pressure on the kinetic curves at 700°C in the case of sample S (synthetic CaCO_3): (a) 533, (b) 800, (c) 933, (d) 1200, (e) 1333 Pa.

order to illustrate the improvement achieved with the present kinetic model.

The expected linear relationship between θ and t was checked from the sets of theoretical and experimental data corresponding to the Fig. 6, and the result is illustrated in Fig. 7. The linear regression coefficient was found to be equal to 0.999 in this experiment. All the values found for the experiments reported in this study ranged from 0.990 to 1.

The specific frequency of nucleation and specific rate of growth were determined in a similar way for various carbon dioxide pressures and samples. The variations of ν and γ are shown in Figs 8 and 9 respectively, as a function of the carbon dioxide pressure. Both the specific frequency of nucleation

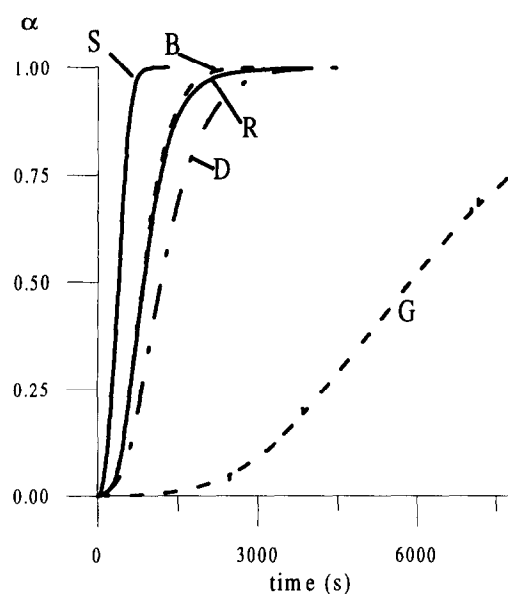


Fig. 3. Fractional conversion versus time at 700°C under 800 Pa of CO_2 for the samples S, G, R, B, D.

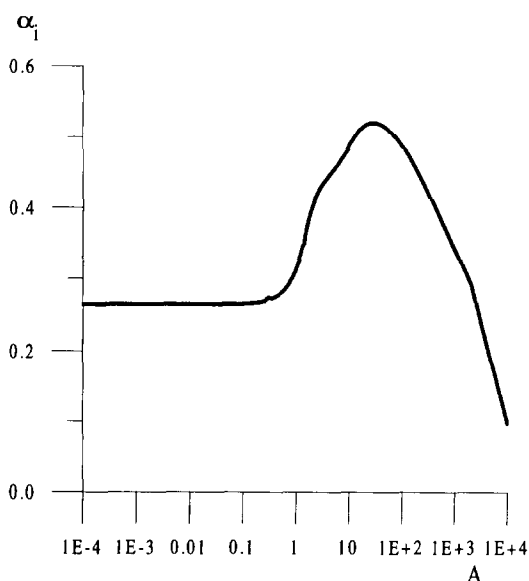


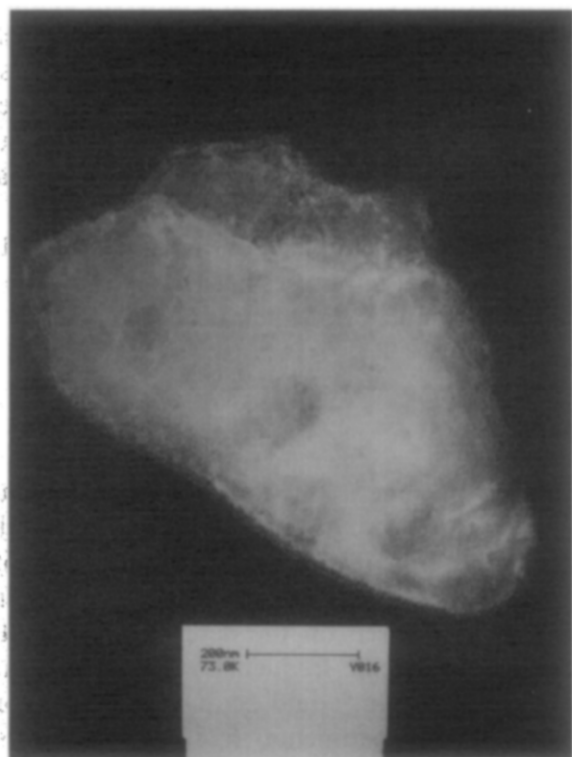
Fig. 4. Variations of the value of the fractional conversion at the inflexion point (α_i) as a function of the parameter A of the kinetic model.

and the specific rate of growth are observed to decrease with increasing carbon dioxide pressure.

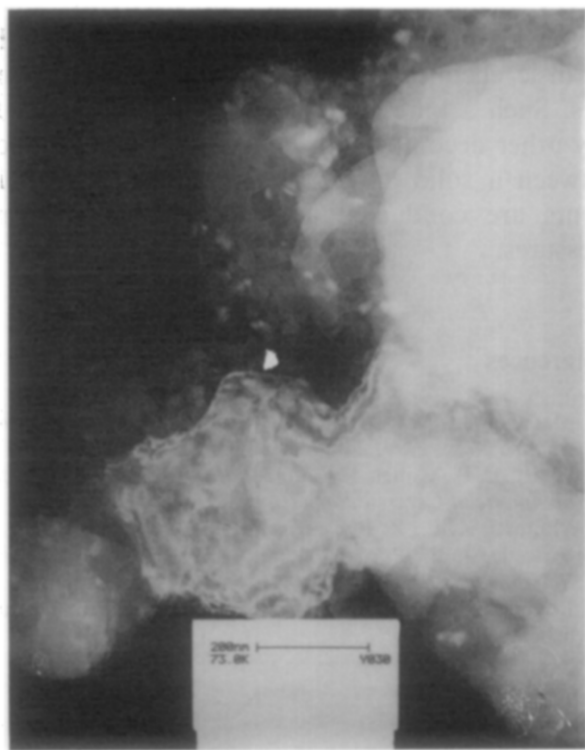
The values of v are not very different from one sample to another since they range from 1×10^{-4} to 6×10^{-4} , at the lowest pressure, and around 0.08×10^{-4} to 0.5×10^{-4} at the highest pressure. On the contrary, the values of γ are strongly different

since we obtain variations by a factor 10^3 from the samples G to S. In addition, the differences observed for v are not related to those observed for γ : this is not surprising since the mechanisms of nucleation and growth are certainly different from the point of view of their elementary steps. It is also interesting to focus on the samples B and R which were found to have the same kinetic curves $\alpha(t)$ (Fig. 3). These two samples can now be distinguished by distinct values of γ and v .

Concerning the influence of the impurities contained in the samples, they are probably responsible for a large part of the differences obtained on the specific frequency of nucleation as



(a)



(b)

Fig. 5. TEM photographs of the sample S decomposed with $\alpha = 0.01$ under 1199 Pa of CO_2 at 700°C : (a) one particle with a single nucleus; (b) several particles partly decomposed.

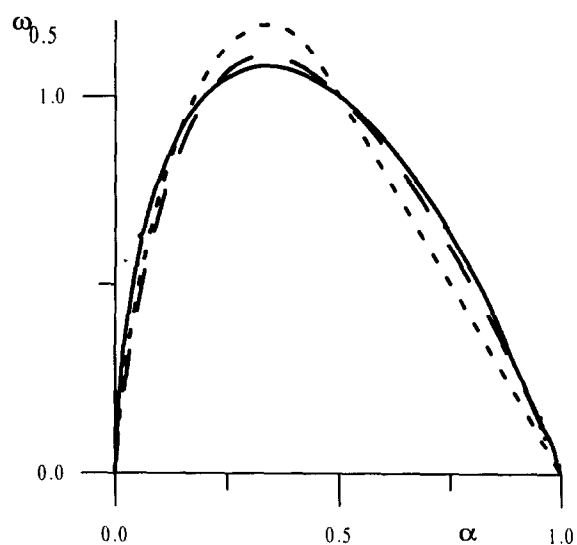


Fig. 6. Comparison of experimental (—) and theoretical reduced rate curves in the case of sample S at 1200 Pa of CO_2 and 700°C : (---) Mampel with $A = 0.8$; (- · -) generalised Mampel with $A = 1.2$.

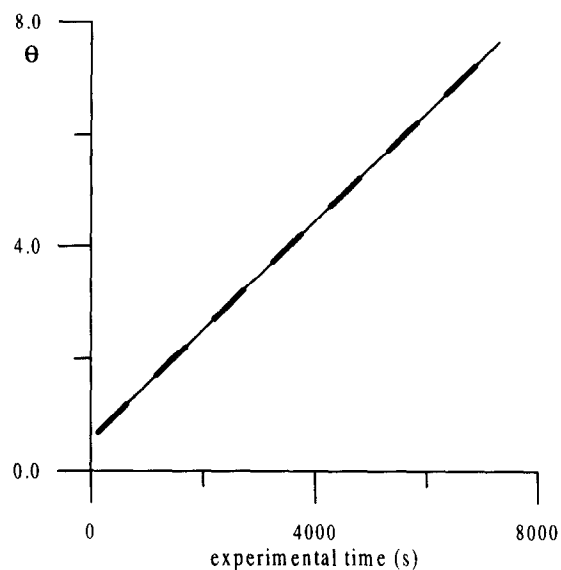


Fig. 7. Relationship between the dimensionless time (θ) and the experimental time corresponding to the result of Fig. 6

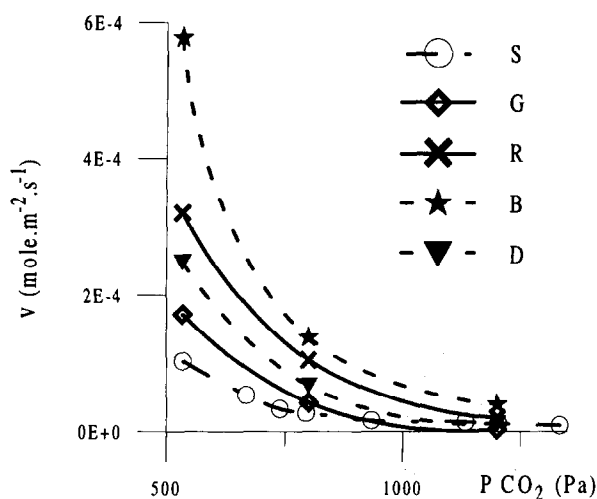


Fig. 8. Values of the specific rate of growth against P_{CO_2} for the samples S, G, R, B, D at 700°C.

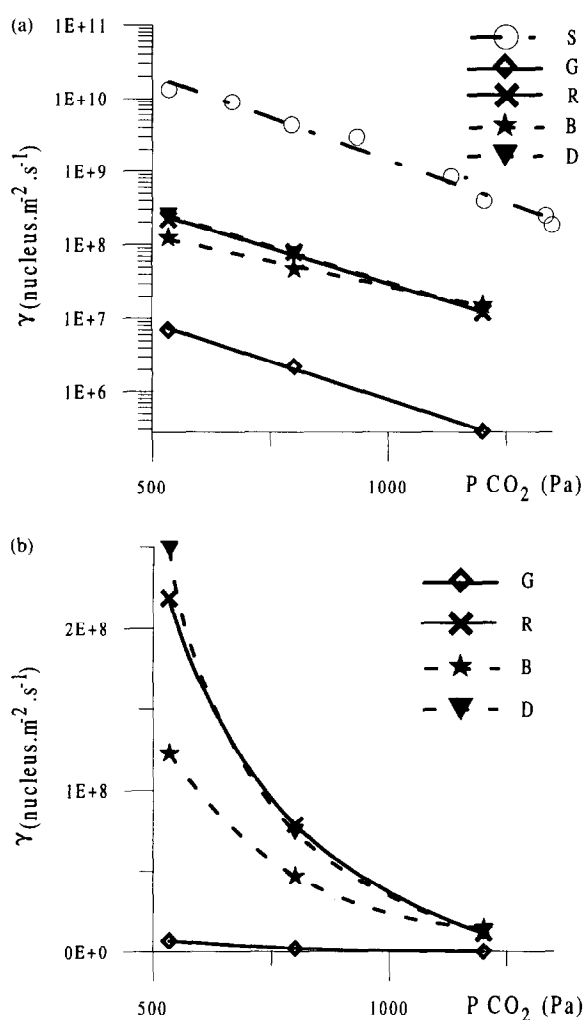


Fig. 9. Values of the specific frequency of nucleation against P_{CO_2} at 700°C for the samples S, G, R, B, D: (a) semi-logarithmic scale, and (b) linear scale.

well on the specific growth rate, although other contributions cannot be discarded, like differences in crystalline faces or surface states. The influence of the impurities is due to their nature and their relative amount, but it is interesting to see that the same impurity may affect independently the specific frequency of nucleation or the specific rate of growth. For example, samples B and D contain the same impurities (cf. Table 1) at a different amount, but their values of γ and v follow an inverted relative order. Moreover in the case of the samples S and R, the same impurities with the same content lead to distinct values of γ and v : this is not surprising since S is a synthetic calcium carbonate whereas R is a natural limestone. It can finally be noticed that the sample G, which contains the lowest amount of impurities has the lowest value of the specific frequency of nucleation.

5 Conclusion

By means of a new kinetic model based on the Mampel's model, we have shown that it is possible to characterise the intrinsic chemical reactivity of a series of calcium carbonate samples. This characterisation is based on the determination of the values of the specific frequency of nucleation and rate of growth. This could be achieved by a comparison of the experimental rate measured in isothermal and isobaric conditions to the theoretical curves deduced from the model. This study revealed a strong effect of the impurities on the intrinsic chemical reactivity of the different samples. Such a kinetic modelling may be applied to any other decomposition reaction or to a reaction between a solid and a gas, provided the experiments are conducted at fixed temperature and pressures.

References

1. Maciejewski, M., Oswald, H. R. and Reller, A., *Thermochimica Acta*, 1994, **240**, 167–173.
2. Hyatt, E. P., Cutler, I. B. and Wadsworth, M. E., *Journal of American Ceramic Society*, 1958, **41**, 70–74.
3. Mampel, K. L., *Z. Phys. Chem.*, 1940, **A187**, 235–249.
4. Viricelle, J. P., Pijolat, M. and Soustelle, M., *J. Chem. Soc. Faraday Trans.*, 1995, **91**(24), 4431–4435.
5. Bouineau, V., PhD Thesis, St Etienne, 1998, to be published.